2009

Chapter 13: Space- and Ground-Based Studies of Lightning Signatures

Timothy Hamlin
Los Alamos National Laboratory

Kyle Wiens

Abram Jacobson

Tracey E. L. Light

Kenneth B. Eack

Chapter 13
Space- and Ground-Based Studies of Lightning Signatures

Timothy Hamlin, Kyle C. Wiens, Abram R. Jacobson, Tracy E.L. Light and Kenneth B. Eack

Abstract This article provides a brief survey of the space- and ground-based studies of lightning performed by investigators at Los Alamos National Laboratory (LANL). The primary goal of these studies was to further understand unique lightning signatures known as Narrow Bipolar Events (NBEs). First, an overview is presented of the Fast On-orbit Recording of Transient Events (FORTE) satellite and of the ground-based Los Alamos Sferic Array (LASA). This is followed by a summary of the phenomenology, physics, and meteorological context of NBEs and NBE-related discharges. This article also discusses additional radio frequency and optical observations of lightning made by the FORTE satellite and concludes with an outlook on LANL's growing interest in the use of lightning observations in the study of severe weather and hurricane intensification.

Keywords Narrow Bipolar Event (NBE) · FORTE satellite · Los Alamos Sferic Array (LASA) · Transionospheric Pulse Pair (TIPP) · Blackbeard experiment · ALEXIS satellite

13.1 Introduction

Los Alamos National Laboratory's (LANL) interest in lightning science began in 1993 when the Blackbeard experiment aboard the ALEXIS satellite began observing unique radio burst signatures of unknown origin. At this time, not much was known about these radio bursts other than that they came in pairs and were far more powerful and of considerably shorter temporal scales than what was usually observed from ordinary lightning. The term transionospheric pulse pair (TIPP) was coined to describe these intense satellite-observed phenomena. Over the last ten years the source of these burst signatures has been identified as a form of intra-cloud

T. Hamlin (✉)
Space and Remote Sensing Group, ISR-2, Los Alamos National Laboratory, Los Alamos, New Mexico, USA
e-mail: thamlin@lanl.gov

H.D. Betz et al. (eds.), *Lightning: Principles, Instruments and Applications*,
DOI 10.1007/978-1-4020-9079-0_13,

lightning. They are often associated with what appears to be a unique class of lightning termed "narrow bipolar events" or NBEs.

This article provides a brief survey of the space- and ground-based studies performed by investigators at LANL in order to further understand the origin of the unique lightning signatures. Section 13.2 describes the Fast On-orbit Recording of Transient Events (FORTE) satellite as well as the ground-based Los Alamos Sferic Array (LASA). Section 13.3 summarizes recent efforts to further understand the phenomenology, physics, and meteorological context of NBEs and NBE-related discharges. Section 13.4 discusses additional radio frequency and optical observations from the FORTE satellite. Section 13.5 presents an outlook for LANL's future role in the study of severe weather.

13.2 Instrumentation

This section briefly discusses two key platforms LANL has used over the last decade in order to further investigate lightning phenomena. The first is the FORTE satellite. The second is the ground-based array of very low frequency/low frequency (VLF/LF) lightning sensors called LASA.

13.2.1 FORTE

The FORTE satellite was launched in August of 1997 and was the second in a series of U.S. Department of Energy research satellites that provided for the study of radio-frequency (RF) and optical emissions from lightning. FORTE is in an 800-km altitude, 70° inclination, circular orbit, and is pointed at nadir. As with its predecessor, the Blackbeard payload aboard the ALEXIS satellite (Holden et al., 1995; Massey and Holden, 1995; Massey et al., 1998a), the FORTE RF payload functioned like a "flying digital oscilloscope". Jacobson et al. (1999) provide a detailed description of FORTE's capabilities, which are summarized in the next subsections.

13.2.1.1 FORTE Antennas

FORTE's large RF antenna structure was supported by a 10-m long nadir-pointing antenna boom. The antenna was deployed two months after launch from its folded storage in the satellite. Along the boom were mounted two passive orthogonal log-periodic antenna arrays designed to point the 25–50 MHz beam-lobe maximum at nadir with the first null of the electric-field-plane lobe at the limb of the Earth (Shao and Jacobson, 2001, 2002). The separation of the antenna's electrical center from the spacecraft, and its intrinsic passive gain, made the FORTE RF signal-to-noise ratio (SNR) much improved over Blackbeard's. The FORTE RF payload achieved background-limited SNR; the background noise in the signal recordings

was dominated by anthropogenic and geophysical sources, and was not limited by spacecraft-generated interference.

13.2.1.2 FORTE's TATR Receiver

FORTE's primary RF receiver was named "TATR" (Twenty megahertz And Twelve bit Receiver) and had two channels with 22-MHz of analog bandwidth each. The base frequency for each channel was selectable from a grid covering the entire high frequency (HF) to very high frequency (VHF) spectrum. The base frequencies of the two TATR channels could be independently selected. When set on the same band, the two channels typically derived their signals from alternate orthogonal antennas. This enabled polarimetry of the incoming signal as described in Shao and Jacobson (2001, 2002) as well as crude direction finding based on antenna-lobe structure (Jacobson and Shao, 2002b). When TATR was set to use different bands on the two channels the combined information was used to examine spectral slope. In either operation mode, the trigger was derived from one channel with the other "slaved" to that trigger. Each channel was digitized synchronously with the other channel with 12-bits of resolution at a rate of 50 megasamples per second. This maintained inter-channel coherence in the recording and enabled coherent polarimetry.

TATR relied upon an eight-channel coincidence trigger. The eight channels were spaced 2.5 MHz apart, and each was 1-MHz wide. The power in each trigger channel was continuously monitored, and the coincident rise of a selectable number of channels above a selectable trigger level caused a trigger signal to be issued. This multichannel trigger design revolutionized the satellite-borne study of lightning RF emissions (Jacobson et al., 1999) because it enabled triggering upon faint pulsed signals which otherwise would be lost in the background (e.g., Lehtinen et al., 2004). The design also prevented undesired triggering by anthropogenic communications signals (Jacobson et al., 1999). In addition to the signal-derived trigger, TATR could be programmed to trigger at a selected time, such as the recording of scheduled illumination by engineered RF pulsers (Massey et al., 1998b).

The powers from TATR's eight multichannel-triggers were continually digitized and stored, even when the TATR systems were not recording events. Burr et al. (2004) used this to produce a global atlas of frequency-resolved VHF noise in the space environment which was unmatched by any other system reported at that time.

During almost six years of operations, FORTE's RF payload recorded over three-million lightning VHF bandpass-filtered waveforms. The vast majority of information was gleaned from the 26 to 48 MHz passband (the so-called "low-band") with an accompanying simultaneous recording either at 118–140 MHz ("high-band") or at low-band but on the alternately-polarized antenna. The signal trigger almost always derived from a low-band channel.

Satellite-borne RF observations suffer from many constraints and complications to which ground-based systems are immune:

1. The propagation path from the lightning emitter to the satellite transits the ionosphere, leading to spectral dispersion of the VHF signal (Fig. 13.2) (Massey,

1990; Massey et al., 1998b; Roussel-Dupré et al., 2001). This is especially severe below 30 MHz, and 20 MHz is the practical limit below which signals from terrestrial lightning cannot be reliably studied by satellite.
2. The satellite views a huge source region for emitters of background noise, against which the lightning signal must compete. As a result, only lightning VHF signals of moderate to high power can be studied.
3. Single-satellite VHF observations cannot straightforwardly locate lightning (Jacobson and Shao, 2001, 2002b; Shao and Jacobson, 2001, 2002). For interpretation of the physical context of the VHF observation, source location is extremely useful. FORTE observing programs were weighted whenever possible toward either joint FORTE VHF/ground-based array observations (Section 13.4.2) or FORTE joint VHF/optical observations (Section 13.4.4).

However, satellite-borne VHF observations have some unique advantages over ground-based systems:

1. Within the limitations of the orbit, satellites offer global coverage.
2. When an intracloud discharge is located by some other means, the recorded RF signal contains information on the emission altitude (Jacobson et al., 2000).
3. Since the satellite is moving and lightning source locations vary, the satellite obtains data from a variety of elevation angles. This diversity of elevation angles facilitates inference of the VHF emission lobe (the lightning "antenna beam pattern") for different lightning processes (Shao et al., 2004, 2005b).

13.2.1.3 FORTE Optical

In addition to its RF instruments, FORTE also had an Optical Lightning Sensor (OLS) on board (Suszcynsky et al., 2001). This included a broadband (0.4–1.1 μm) silicon photodiode detector (PDD) and a charge-coupled device imager, called the Lightning Location System (LLS). OLS data were Global Positioning System (GPS) time-stamped to a precision of 1 μs. The FORTE/OLS field-of-view was 80°, providing a 1200-km diameter footprint on the Earth below.

The PDD allowed for excellent temporal resolution of optical lightning emissions at 15 μs per sample, but could only geolocate events to within its footprint. The PDD could be operated such that it triggered autonomously when a signal was detected that rose above a noise-riding threshold level, or it could be triggered in a "slaved" mode where it recorded data whenever the LLS triggered. Record lengths were either 1.92 ms (autonomous) or 6.75 ms (slaved). The LLS offered complementary information, in that it geolocated events to within 10 km and provided two-dimensional imagery, but only sampled the light at 2.5 ms intervals. The LLS front-end operated autonomously and included a narrow band 777.4 nm spectral filter.

Note, there are two additional articles in this text which discuss space-based optical lightning measurements; see also: Adamo et al. (this volume) and Finke (2009).

13.2.2 The Los Alamos Sferic Array

Since its construction in 1998, the Los Alamos Sferic Array (LASA) has been in continuous operation. LASA is a network of electric field change meters that was originally built to provide support and ground-truth for the FORTE mission. Over time LASA has been used as a collaborative tool not only for FORTE, but also for providing ground-truth support to VHF observations by orbital receivers aboard the GPS satellites (Suszcynsky et al., 2005). In addition to the joint studies, LASA has demonstrated great utility as a stand-alone resource for performing lightning investigations.

By recording arrival times of lightning electric field change sferics at multiple geographically-distributed sensors and taking the difference between unique combinations of pairs of these arrival times, the location of the lightning discharge can be calculated via time difference of arrival techniques. Note that we use the term "sferic" as a colloquialism of the word *atmospheric:* the remotely-observed transient electric field change produced by lightning. The magnitude and sign of the measured electric field change are used to deduce physical properties of the discharge, such as peak current, polarity, and type of lightning. Smith et al. (2002) characterized the location accuracy of the LASA by comparison with the National Lightning Detection Network (NLDN: Cummins et al., 1998), and found it to be approximately 1 km for sources inside the array of stations.

The initial configuration of LASA consisted of five flat-plate "fast" electric field change sensors distributed across the U.S. state of New Mexico. The LASA expanded to 11 stations by 1999 (four in New Mexico, one in Texas, one in Nebraska, and five in Florida). See Smith et al. (2002) for a more complete description. As described by Shao et al. (2006), the LASA sensor hardware and trigger design were recently improved. A set of these improved sensors was deployed in Florida in 2004, and a second set of improved sensors was deployed in the U.S. Great Plains in 2005. Wiens et al. (2008) provides a detailed analysis of the performance of the improved Great Plains LASA. At present, LASA sensors use a 1 ms time constant and digitize the 0.2–500-kHz filtered output voltage change waveforms from the fast antenna circuit/flat plate antenna at 1 MHz with approximately 15 bits of resolution. The LASA sensors utilize a software-controllable floating bipolar event trigger. The record length for each triggered event varies but is usually between 1.5 and 3 ms. Time stamping is achieved via a GPS receiver and is accurate to roughly one microsecond.

13.3 The Characteristics of Narrow Bipolar Events

NBEs are a distinct class of intra-cloud (IC) lightning discharges first detected and reported by Le Vine (1980) and Willett et al. (1989), and described in more detail by Smith et al. (1999). The term "NBE" is derived from the phenomenological description of the sferic based on its VLF/LF waveform. NBE is perhaps not the best descriptive term for these discharges because any discharge involving a current that

turns on then off will produce a bipolar waveform in the radiation zone. However, NBE sferics are distinguished uniquely from ordinary cloud-to-ground (CG) and IC lightning sferics by their narrow (∼10-μs) bipolar pulse widths, high SNR values, and their temporal isolation from other lightning-related field changes. For example, Fig. 13.1 shows two 500-μs-long recorded NBE sferic waveforms detected by a LASA sensor from a range of approximately 500 km. The upper panel shows a typical positive NBE (+NBE), and the lower panel shows a typical negative-polarity NBE (–NBE).

There is strong phenomenological evidence that NBEs are co-located and occur simultaneously with sources of strong VHF emissions, such as the so-called TIPPs. Ground-based observations (Le Vine, 1980; Willett et al., 1989; Smith et al., 1999; Thomas et al., 2001) and space-based observations with FORTE (e.g., Jacobson et al., 2000; Jacobson and Light, 2003), and observations from an experimental receiver aboard a GPS satellite (Suszcynsky et al., 2005) have shown that NBE-related

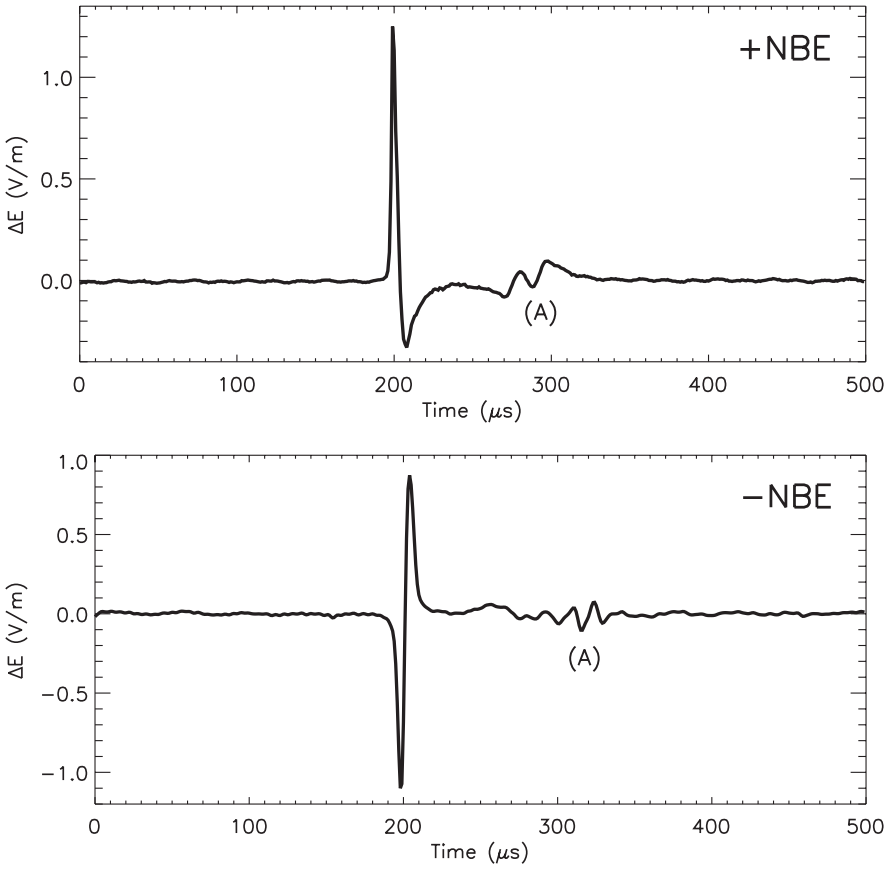

Fig. 13.1 Example sferics from a +NBE (*top*) and –NBE (*bottom*). Labels "(A)" show the ionospheric and ground-ionospheric reflections like those used by Smith et al. (2004) to determine the intracloud discharge source height as well as the virtual ionospheric reflection height

processes emit the most powerful pulses of VHF radiation produced by lightning. They constitute the majority of VHF lightning emissions detected from space at GPS orbit. Hence, Suszcynsky and Heavner (2003) have identified NBEs and NBE-related processes as the "primary target of opportunity for future satellite-based VHF global lightning monitors."

It is important to make a distinction between the NBE sferic observed at VLF/LF and the strong VHF pulses associated with NBEs. It is not yet clear that both components always occur together (Jacobson, 2003a). However, for brevity, we will loosely apply the term "NBE" to describe the overall discharge process observed at any frequency.

13.3.1 Ground-Based Observations of NBEs

13.3.1.1 Electrical Characteristics

Smith et al. (1999) collected some of the first detailed ground-based measurements of +NBEs made by LANL. Among their results are: (1) peak +NBE electric field change amplitudes are comparable to those of return strokes, (2) the amplitudes of HF/VHF emissions from NBE-related discharges are approximately 10 times greater than those from normal lightning, (3) NBEs are compact in both time and space ($\sim$10 μs pulse widths, and less than 1 km in length).

NBE waveforms typically contain smaller amplitude pulses that lag the initial pulse (Smith et al., 2004). See, for example, the features labeled "(A)" in Fig. 13.1. These delayed pulses are due to ionosphere and ground-ionosphere reflections of the NBE skywave. Such reflection signatures are further evidence that NBEs are elevated sources (i.e., intra-cloud), and when combined with the horizontal location of the source the time delays of these pulses provide both the emission altitude of the NBE as well as the virtual reflection height of the ionosphere.

When observed by broadband field change antennas from large distances, NBEs exhibit their characteristic bipolar radiation field waveform. When observed at close range (less than ten kilometers), NBE's electrostatic and inductive field changes can often be observed in addition to the bipolar radiation field change in their electric field change records. LASA measurements in 1998 and 1999 located NBEs of both positive- and negative-polarity, a small number of which were located within 10 km of one of the ground stations. For these events, the dipole moment change could be determined directly from the electrostatic field change in combination with the independently-measured radiation field change from a distant station. This allowed for the average propagation velocity to be determined by equating the two dipole moment change determinations; one in the static- and the other in the radiation-zone. From this, the length of the discharge was estimated using the velocity and the duration of the event. Additional details about these calculations can be found in Eack (2004), who determined that on average, a NBE transfers 0.3 C of charge over a distance of 3.2 km, and that the discharge wave-front propagates at an average speed equal to one-half the speed of light (similar to that of return-strokes). The average current was 16 kA, with a peak current as high as 29 kA measured for one NBE.

Hamlin et al. (2007) describe another technique for determining the spatial extent of NBEs. In a dataset consisting of 133 +NBE lightning discharges located by LASA, Hamlin et al. investigated a secondary positive peak that occurred in each record that followed the primary positive peak in the +NBE waveform. The secondary peak was a small positive perturbation in the negative trough of the otherwise ordinary NBE waveform. The perturbation was seen at multiple LASA stations per event and is co-located with the primary NBE discharge source. The secondary peaks are not to be confused with the signatures from ground or ionospheric reflections. In fact, the results were shown to be consistent with what would be expected for a propagating current pulse reflecting off an impedance discontinuity along a transmission line. With an assumed propagation speed, the time difference between the primary and secondary (assumed to be the reflected) peak in the field change record offered a direct technique for estimating the (presumed vertical) length of the discharge channel. The technique, analogous to measuring the length of a transmission line via time domain reflectometry techniques (except in the radiation-zone rather than along the conductor itself) was used to find the upper-limit-length for NBE discharge channels. Bounded by the speed of light, the limit on channel length for the typical positive narrow bipolar event was shown to be approximately 2 km. This value was twice the estimate by Smith et al. (1999) and about two-thirds the 3.2 km reported in Eack (2004) and can be considered a refinement of the original length estimates. The study also used the ratio of the primary-to-reflected signal amplitudes to obtain an attenuation coefficient. Using this, a temporal decay constant of approximately 4 μs was found for +NBEs. Assuming a propagation speed of one-half the speed of light the temporal decay constant translates to a spatial decay scale length of $\sim$600 m (i.e., the conductive-length of the channel decays from its initial value to "1/e" of this in about 600 m).

13.3.2 FORTE Observations of NBEs

By definition, a NBE sferic is the unique waveform signature observed at VLF/LF frequencies. However, an intense burst of noise is also often observed simultaneously at higher frequencies. The power of the higher-frequency noise is essentially constant versus frequency through FORTE's the range of VHF frequencies. The original observations of NBEs by Le Vine (1980) included simultaneous recordings of both the sferic and the HF noise, and he noted that the HF signal appears like a noise burst added to the sferic which lasts a few microseconds. That is, the HF/VHF noise is not a coherent extension (to higher frequencies) of the basic sferic waveform. Le Vine's data could not constrain the emission height of the sferic or the HF noise pulse.

Blackbeard's VHF receiver lacked a multichannel coincidence trigger and required a high trigger threshold. As a result, Blackbeard could be triggered by only the most intense lightning phenomena. What Blackbeard recorded were almost always the same sort of intense pulses described in Le Vine (1980) as the noise burst accompanying the sferic. However, the Blackbeard observations systematically

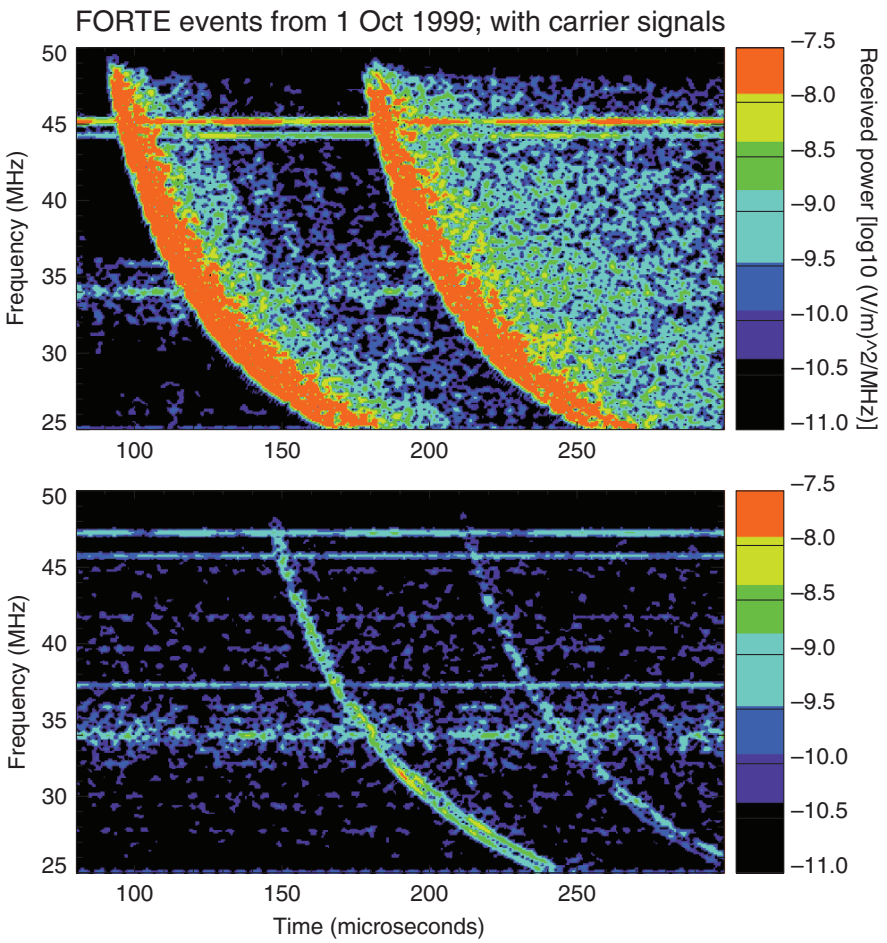

Fig. 13.2 Spectrograms of a (top) strong intracloud pulse typically associated with a VLF NBE and (bottom) a weaker polarized/coherent intracloud pulse. Note the difference in pulse width and strength between the two events, as described in Jacobson and Light (2003). The ionospherically-induced, frequency-dependent dispersion is evident in the graphics, as well as the geomagnetic splitting (most visible in the lower panel at the lower frequencies of the primary signature). In addition to the lightning signals, one can discern interference from anthropogenic radio transmissions, apparent as narrow, horizontal bands. In each spectrogram, the ground-reflection accounts for the echo which occurs approximately 50–75 μs after the primary pulse (See also Plate 17 in the Color Plate Section on page 603)

revealed a second pulse, or the "pulse pair" in the term TIPP. Statistical study of the second-pulse delay times suggested strongly that the second pulse was a ground reflection of the first pulse rather than a physically delayed second emission process (Holden et al., 1995; Massey and Holden, 1995; Massey et al., 1998a). This is not inconsistent with Le Vine's original single-pulse HF recording as a ground-based receiver would not see a distinct second pulse (Jacobson et al., 1999).

FORTE results on their own (Jacobson et al., 1999), as well as the joint FORTE and NLDN campaign (Jacobson et al., 2000), definitively confirmed the Blackbeard inference that the second pulse in a TIPP was merely a ground reflection of the first pulse. The inferred height of the TIPP pulses and the sferic, determined via altogether different data and methods but on simultaneous and common events, agreed to within ∼2 km; this was consistent with the height-determination error from Smith et al. (2004). Moreover, the sferic and VHF signals were simultaneous to within the timing uncertainty (∼1 μs). Figure 13.2 shows two example TIPPs detected by FORTE. The top panel shows a "strong" intracloud pulse typically associated with a VLF NBE. The bottom panel shows a weaker intracloud pulse. Both types of pulses occur in pairs at the FORTE satellite; the delayed second pulse of each pair is the reflection from the earth's surface.

13.3.2.1 Weak Versus Strong RF Pulses

FORTE's RF data led to several robust findings about the characteristics of VHF pulses originating from IC discharges. The overall picture was that IC pulses diverged broadly into two categories: weak or strong in effective radiated power (ERP). An ERP of ∼40 kW (integrated over the FORTE low-band; 26–48 MHz) appears to be a dividing region, on either side of which FORTE IC pulses have distinctive behaviors. Those with ERP $\ll$ 40 kW are categorized as weak, polarized, narrow, and coherent pulses, while those with ERP $>$ 40 kW are in the broader and incoherent "strong IC pulses" category (see also, Figure 13.2).

With regard to their polarization characteristics, the weak pulses are linearly polarized while the strong pulses are less polarized; more work is required to clarify whether their polarization is random or something more organized. Waveform coherence is related to the ratio of the pulse-width to the inverse of the signal bandwidth, i.e. coherence may be quantified by the "time-bandwidth product". The weak pulses tend to have time-bandwidth products of roughly unity, while the strong pulses have products much larger (i.e., the strong pulses are extended wave trains of noise). Thus with regard to waveform coherence, the weak pulses tend to be perfectly coherent, while the strong pulses appear to be incoherent. We summarize the two archetypes' widely differing characteristics as follows (Jacobson, 2003a, 2003b; Jacobson and Light, 2003):

1. Emission intensity: Those categorized as strong pulses have intensities that are two (and sometimes three) orders-of-magnitude greater than the weaker polarized/coherent pulses.
2. The strong pulses are randomly polarized, whereas the weaker polarized/coherent pulses show linear polarization.
3. The strong pulses are either isolated in time, or serve as initiators of flashes whose subsequent emissions are not as strong and are frequently polarized/coherent. In contrast, the weaker polarized/coherent pulses can occur anywhere in an IC flash and are not uniquely observed as initiators of flashes.

The weaker polarized/coherent pulses are usually accompanied closely in time by other pulses of the same type.

4. The strong pulses show deep frequency-dependent fading within the pulse, whereas the weaker polarized/coherent pulses have a simple, coherent monopulse structure.
5. The strong pulses are very wide compared to the weaker polarized/coherent pulses (~3–5 μs versus ~0.1 μs).
6. The strong pulses are the RF pulses seen with simultaneous NBEs recordings of the radiation-field vertical electric field sferic near the ground. By contrast, the weaker polarized/coherent pulses have no special simultaneity or preferred association with NBEs.
7. In storms that produce both strong RF pulses recorded by FORTE and NBE field changes recorded by LASA, there are always more strong RF pulses than NBEs. It appears that strong RF pulses can occur without an associated NBE, but NBEs are always accompanied by strong RF pulses (Jacobson, 2003a).
8. Storms containing strong RF pulses along with coincident NBE field changes have few if any flashes. That is, NBE-coincident strong pulses are more isolated from neighboring lightning activity than are strong pulses lacking coincidence with a NBE sferic.
9. In storms containing lightning flashes that are initiated by strong RF pulses, and in which both FORTE and LASA could observe the same storm, there are almost never NBEs.
10. In flashes that are initiated by strong RF pulses, the subsequent leader-like pulses in the flash tend to occur at higher altitude than where the flash is initiated by the strong RF pulse.
11. In flashes that are initiated by strong RF pulses, optical concurrence tends to occur only for subsequent pulses (if at all) and tends not to occur for the initiator strong RF pulse.
12. The strong RF pulses in a given storm appear to have a truncated ERP distribution, staying below a limiting ERP. For most storms this ERP limit is on the order of 1 MW peak, integrated over the FORTE low-band of 26–48 MHz.

13.3.2.2 Optical Signatures and NBEs

Light and Jacobson (2002) examined the joint optical and RF data from the specific class of lightning detected and classified by FORTE as "impulsive intracloud VHF events". These impulsive events comprised 47% of the FORTE VHF data overall. However, in the sub-set of events that comprised the most powerful VHF events (those likely to have VLF/LF NBE counterparts) the "impulsive" events were over-represented and accounted for 60–70% of the data. Light and Jacobson showed that, in general, as the detected VHF peak power increased, the likelihood of optical coincidence similarly increased. A surprising finding, however, was that in the NBE-corresponding class of very-powerful, impulsive VHF events, the likelihood of optical coincidence was inversely proportional to the peak VHF power. The data showed a transition point in power where the optical coincidence rate continued

to climb for all types of events, except VHF-impulsive events which dramatically begin to lose their optical counterparts. This led to the suspicion that the strongest impulsive VHF events may be a distinct class of discharge, which produces little or no optical emission. This new finding of "dark lightning" has yet to be explained. We do no yet know whether there truly is no optical emission at all from NBEs or if it is just a detection/sensitivity issue. All we know presently is that the optical emission is below the detection threshold of current instruments. Unpublished data have shown agreement with the "dark lightning" finding, in that photodiodes fielded alongside ground-based VLF/LF sensors typically show no optical light curves detected from corresponding VLF/LF NBE detections. Therefore, the upper limit to radiated power of any NBE-optical-emission appears to be low.

13.3.3 The Meteorological Context of NBEs

Research at LANL has established the basic meteorological context of NBEs. A survey of the publications from this research reveals that some of the observed characteristics of NBEs are consistent from one study and geographical region to the next. However, there are also inconsistencies. The key points may be summarized as follows:

NBEs occur in the same general meteorological context as other lightning, that is, within or near the convective cores of thunderstorms (Smith et al., 1999; Suszcynsky et al., 2005; Jacobson and Heavner, 2005). NBEs have been observed in air mass thunderstorms and frontal storms (Smith et al., 1999; Shao et al., 2006) in severe multi-cell and supercell storms (Tessendorf et al., 2007; Wiens et al., 2008) as well as in tropical cyclones (Suszcynsky et al., 2005). Though NBEs occur in the same storms as other lightning, they tend to occur in relative temporal isolation from other lightning, i.e., not as part of ordinary lightning flashes. When they do occur as part of a flash, they usually initiate the flash, and their emission altitudes are in the same general range (10–15 km) as ordinary IC flashes (Rison et al., 1999; Jacobson, 2003a, 2003b; Jacobson and Heavner, 2005; Smith et al., 1999, 2004). Indeed, Jacobson and Heavner show that NBE emission altitudes are generally constrained to below the height of the tropopause.

NBEs constitute a small percentage of all lightning discharges (probably much less than 1%). Table 13.1 lists the percentage of NBEs relative to other lightning observed in several recent studies. These percentages should be treated as very rough estimates because the NBE percentage is difficult to quantify. Total lightning itself is not a readily measured (or measurable) quantity, especially when large spatial and temporal domains are considered. The percentages in Table 13.1 are overestimating the NBE percentage because the total lightning counts are underestimated (see, for example, Wiens et al., 2008). Furthermore, the instrumentation used to observe NBEs and other lightning varies from one study to the next, as does the geographical region.

The majority of NBEs observed are positive-polarity (Table 13.1). The percentage of +NBE relative to all NBEs observed varies from study-to-study and also

Table 13.1 Percentage of NBEs observed relative to all lightning observed and percentage of all NBEs observed that were of positive-polarity. Results are listed by study and by geographical region

Study	NBE (% of all)	+NBE (% of NBEs)
Smith et al. (2002)		
New Mexico Only	0.63	84
New Mexico and Florida	1.57	70
Suszcynsky and Heavner (2003)		
Florida	N/A	65
Jacobson and Heavner (2005)		
Florida	3.35	76.6
Wiens et al. (2008)		
Great plains	0.5	77

by geographical region (New Mexico versus Florida versus the Great Plains), but +NBEs are consistently more common. Smith et al. (2004) found that the distribution of NBE emission source heights is roughly bimodal, with a lower mode near 13 km associated with +NBEs and an upper mode near 18 km associated with –NBEs. These collective results are consistent with the idea that +NBEs are intra-cloud discharges that initiate between the main negative and upper-positive charge regions of the commonly observed tripolar charge configuration of thunderstorms. In fact, Rison et al. (1999) show a specific example of a +NBE initiating a normal intra-cloud discharge in a tripolar thunderstorm. Perhaps the less common –NBEs are discharges that initiate between the upper-positive and an additional overlying negative charge region, possibly a screening layer charge. Or perhaps the –NBEs are indicative of storms with an elevated charge structure, or even an inverted tripole charge structure. In their statistical study, Jacobson and Heavner (2005) found that Florida storms rarely produce both polarities of NBEs, while Wiens et al. (2008) found that Great Plains storms often do produce both polarities. Great Plains storms differ from storms elsewhere in the U.S. in many ways, such as severity, ground flash polarity, and charge structure (e.g, Lang et al., 2004; Rust et al., 2005; Wiens et al., 2005). Perhaps the difference in NBE production in Great Plains versus Florida storms is another manifestation of the difference in the storms themselves.

In a statistical sense, the NBE rate is correlated with the total lightning rate. We must stress that this is true only in a statistical sense, not necessarily in any given storm. This relationship between NBE rate and total lightning rate also appears to vary according to the geographic region. For example, Suszcynsky and Heavner (2003) found a significant positive correlation (with large variance) between NBE rates and CG flash rates in Florida storms when considering a large sample of storms. However, there were many storms in their sample which produced CG flashes but did not produce any NBEs. In comparison, Wiens et al. (2008) found a weaker (but still positive) statistical correlation between NBE rates and total lightning rates for storms of the Great Plains. Wiens et al. (2008) also found

that most thunderstorms do not produce NBEs. This leads to the following general observations about NBE phenomenology:

1. NBEs do not seem to occur in all thunderstorms. For those storms that do produce NBEs, the NBEs tend to cluster more closely in both space and time than does other lightning. Strong evidence of this clustering may be found in the statistical studies of both Jacobson and Heavner (2005) and Wiens et al. (2008). Individual case studies also show this NBE clustering (e.g., Smith et al., 1999; Suszcynsky et al., 2005; Tessendorf et al., 2007; Wiens et al., 2008). For example, in one of the storms they studied, Smith et al. noted that the NBEs occurred in sporadic clusters during relatively intense periods of thunderstorm activity. In comparison with the lightning in general, the NBEs were more highly confined to a small region centered on the high radar reflectivity core.
2. It may be that NBEs are indicative of specific types of storms and/or a specific phase of storm development. There is some circumstantial evidence that NBEs are indicative of stronger storms (storms with rapidly increasing or extreme convective strength), and that weaker storms do not produce any NBEs at all. Recall that Suszcynsky and Heavner (2003) found many cases in which Florida storms produced CG flashes but no NBEs. These cases were largely associated with low CG flash rates, suggesting that only the stronger storms produced NBEs. To investigate whether NBEs were indicative of stronger storms in the Great Plains, Wiens et al. (2008) binned their observations into 20-km by 20-km by 10-min space-time cells and then separated these binned observations into two statistical sub-samples: space-time cells with lightning of any kind, and space-time cells with at least one NBE. The cells containing at least one NBE were much more convectively intense than those without any NBEs. In the statistical median, the maximum radar reflectivity was 11–13 dBZ larger, the maximum 30-dBZ altitude was 4–5 km higher, and the total lightning flash rate was an order of magnitude greater. Furthermore, Wiens et al. found that the probability that a cell contained a NBE increased within the increase of every measure of convective strength they considered. They cautioned, however, that even the strongest convection did not always produce NBEs.

13.4 Other FORTE Lightning Observations

13.4.1 Emission Height for Intracloud VHF Emitters

A VHF pulse propagates from an above-ground lightning emitter to the satellite along two distinct paths: the direct path to the satellite and the ground-reflected path, which is longer. The added length of the ground-reflected path causes that path's contribution to the received signal to be delayed relative to the direct path. If the emitter's latitude and longitude are known, e.g., from a lightning-location array's simultaneous detection of the same event, then the VHF recording can be used to infer the emission height (Jacobson et al., 1999, Tierney et al., 2002). This was

done automatically for hundreds of thousands of FORTE recordings of intracloud pulses. The primary pulse usually derives either from leader-step-like discharges or from much more powerful emissions associated with NBEs. Occasionally a TIPP can be formed by an exceptionally brief ($\sim$10 μs) intracloud streamer discharge, such as seen in association with positive cloud-to-ground (CG) discharges (Jacobson et al., 2000).

13.4.2 Coordinated Campaigns with Ground-Based Arrays

FORTE observations were coordinated region-by-region so as to maximize triggered recordings where there was also coverage by various lightning-location arrays. The most extensive coordination was with the National Lightning Detection Network (NLDN) circa 1998–2000, and resulted in a comprehensive understanding of the relationship of space-borne VHF and ground-based LF detection, both in terms of trigger relative biases and detailed timing differences between the VHF and LF emissions (Jacobson et al., 2000). The FORTE/NLDN coordinated campaign established the following:

1. NLDN-FORTE coincidences which rise above the accidental coincidence level are prompt to within $\sim$30 μs.
2. FORTE-observed VHF emissions in the North America sector are often as strong as, or stronger than, Blackbeard-observed TIPPs.
3. Satellite-observed VHF emissions are much more likely to be associated with intracloud discharges than with cloud-to-ground discharges.
4. Satellite-observed VHF emissions are more likely to be associated with positive- than with negative-cloud-to-ground discharges.
5. Satellite-observed VHF emissions associated with intracloud discharges tend to be narrower in pulse-width than are VHF emissions associated with either polarity of cloud-to-ground discharges.
6. TIPPs that are associated with NLDN discharges display a region-dependent emission-height distribution, suggestive of the height-versus-latitude dependence of key isotherms, e.g. -20°C, in the troposphere. Over the Continental U.S./Canadian interior above 45° N, the half-points of the distribution are at roughly 6 and 9 kilometers, and the peak is at 7–8 km. Over the southern maritime region, the peak is at $>$ 13 km, and the distribution is broader. There is no statistically significant evidence, among the TIPPs that are associated with NLDN discharges, for TIPP-emission heights above 15 km.

In addition to the NLDN study, there were intensive campaigns involving joint FORTE-VHF recordings with other lightning-location systems. These included the United Kingdom Meteorological Office's array (Lee, 1986a, 1986b), LASA (Smith et al., 2002) and the World Wide Lightning Location Array (Lay et al., 2004; Rodger et al., 2004, 2005).

13.4.3 Negative Cloud-to-Ground Discharges Over Sea Water

The joint campaigns with both NLDN and LASA allowed FORTE to identify a unique VHF emission associated with the contact of the downward stepped leader with seawater (Jacobson and Shao, 2002a, Shao et al., 2004, 2005b). This species of especially narrow sferic pulse (∼100 ns) had been seen by early ground-based observations (Willett et al., 1990, 1998; Willett and Krider, 2000). The FORTE-sferic array campaigns established some interesting characteristics of the VHF radiation for a negative CG on seawater:

1. The VHF signal from a negative CG on seawater is simply a coherent extension of the sferic waveform. Because of this, the spectral roll-off is much steeper than for the noise-like strong intracloud VHF emissions.
2. By combining data from VHF recordings when the satellite was at various elevation angles (as seen from the discharge), the antenna beam lobe of the VHF emission could be inferred statistically (Shao et al., 2005b). The lobe is oblique-upward beamed, unlike a simple horizon-directed dipole pattern. The oblique-upward beaming is consistent with the field being radiated by an upward moving current front moving at 75% of the speed of light (in the leader-prepared channel).
3. The radiated VHF field is perfectly linearly polarized, as expected from a single vertical emitter.
4. The emission lobe is inconsistent with a "bidirectional leader" model, which has been proposed in the past for the ground-connection process in a negative CG discharge (see discussion in Section 5 of Shao et al. (2005b)).
5. The 100-nanosecond-duration sferic is radiated from a vertical extent of no more than 20 m in height.

13.4.4 FORTE Optical Observations

13.4.4.1 Comparison with NLDN

Kirkland et al. (2001) compared FORTE's photodiode detector (PDD) observations with the NLDN. They found a PDD detection efficiency of ∼6% for individual NLDN-reported cloud-to-ground strokes and a ∼23% detection efficiency for NLDN-reported flashes, which contain ground strokes. The flashes detected by both PDD and NLDN included only 8% of the PDD data, leading to the interpretation that the PDD was sensitive to a far greater fraction of in-cloud discharges, whereas the NLDN is known to predominantly detect (or at least record) ground strikes. The detection efficiency was only marginally higher for positive-polarity CGs compared to those of negative-polarity.

13.4.4.2 Discrimination of Lightning Type

A comparison of FORTE RF and FORTE optical data was first presented in Suszcynsky et al. (2000). In that work, the authors considered the potential for "fingerprinting" the type of lightning discharge according to its VHF time series structure. For example, initial, negative-polarity return strokes are readily identifiable because the intense emission that accompanies the attachment of the channel to ground is preceded by many milliseconds of increasingly strong VHF spikes, presumably from stepped leader activity, superimposed on a rising background, and an abrupt return to original VHF noise levels shortly after attachment. In all, six types of discharges were described in that work: (1) initial, negative return strokes with stepped leader; (2) subsequent negative return strokes, sometimes showing evidence of dart leader; (3) initial positive return strokes; (4) impulsive in-cloud discharges; (5) non-impulsive in-cloud discharges; and (6) mixed IC (with both impulsive and temporally broad emission, combined) .

Light et al. (2001) used the VHF classification scheme of Suszcynsky et al. (2000) to explore the optical characteristics of VHF-detected lightning for each discharge type. It was shown that, in general, RF peak power and optical peak irradiance were broadly correlated. Both the VHF and optical emission were weaker for in-cloud discharges of any type, compared to ground strokes; ground strokes were also approximately 30% more likely to have coincident VHF-optical signals than were in-cloud events, regardless of event peak power. The correspondence between optical and VHF emissions for initial negative return strokes was much greater than for any other type of lightning (Light et al. 2001 looked only at events within a common field of view of both the optical and VHF sensors): every one detected and identified in the VHF data also had a coincident optical signal. The difference in peak VHF power between these events and other types of ground strokes was not significant, although they were the strongest optical detections by a factor of two to five. Therefore this high VHF/optical coincidence rate is not simply an effect of these discharges being generally strong, but rather is intrinsic to the nature of initial negative-polarity return strokes. The question of whether one can ascertain the lightning discharge type on the sole basis of optical emission was addressed by Davis et al. (2002). Again, optical waveform characteristics were found to be statistically slightly different among the assorted lightning types, but not such as to allow individual event discrimination. The greatest peak optical power, on average, arose from waveforms associated with positive-polarity ground strokes, which also showed greater effective pulse widths by 30–50%.

13.5 LANL and the Study of Severe Weather

Many types of extreme weather that cause loss of life or crop and structure damage (tornadoes, flash floods, hail and lightning) are generated by late-stage, severe convective storms. The transition from "regular" to "severe" weather has

been associated with a rapid increase or "jump" in the lightning activity (Williams et al., 1999). Improved early warning methods, including efficient detection and tracking of intense-convection cells through lightning activity by systems like the LASA could help to mitigate some of the effects of these storms. For example, studies of lightning as a precursor to severe weather indicate that tornado-related deaths can be reduced by 20% with the improved warning lead time gained through lightning monitoring (Weber et al., 1998).

It was previously thought that another serious weather-related threat, namely hurricanes, did not reveal itself through lightning intensification. However, during the deadly 2005 hurricane season LASA observed abundant lightning activity within hurricanes Katrina, Rita, and Wilma (Shao et al., 2005a). The vertical ascent of the lightning discharge emission sources can be used as a proxy for convective-cell development and, through this, it may be possible to use lightning to gauge the likelihood of severity increase. A demonstration of this occurred when LASA-detected lightning activity from Rita peaked as the hurricane transitioned from Category 3 to 5 (Shao et al.). These observations of the lightning in the hurricane eyewall region have motivated recent LANL efforts to discover, investigate, and monitor the convective activity in the critical eyewall region.

The great uncertainty in hurricane intensification forecasting is the prediction of the intensification triggering mechanism, thought to be small-scale violent convective events in the eyewall known as "vortical hot towers". Current observational techniques do not allow for continuous real-time observations of vortical hot tower formation. However, systems like LASA can, in principle, provide continuous, all-weather, remote monitoring of eyewall processes with high spatial and temporal accuracy. LANL is in the process of deploying a new high-density dual-band (both VLF/LF and VHF) LASA network in the Gulf of Mexico which is hoped to provide maps of the developing lightning-source regions inside individual convective towers, as well as information about the overall charge structure and flash rate.

LANL also operates a constellation of VHF sensors which are a payload on the GPS satellites. The same VLF/LF NBEs that offer severe-storm monitoring capabilities on the ground also comprise a significant portion of the VHF lightning signals detected by these sensors in orbit (Suszcynsky et al., 2005). Thus, the GPS-based receiver constellation has the capability to eventually offer real-time convection tracking and storm assessment across the globe.

Acknowledgments This work was sponsored by the Department of Energy/National Nuclear Security Agency (DOE/NNSA). The FORTE RF payload functioned for almost six years, three times longer than the expected mission lifetime. This extraordinary longevity was the product, in part, of the robust design architecture by satellite-development leader S. Knox and his team and also due to the scrupulous on-orbit maintenance and resourceful problem-solving skills of the mission-operations leaders D. Roussel-Dupré and P. Klingner. The success of LASA's design, deployment, and long-term operations and maintenance is due to a long list of people and institutions, to whom we owe an enormous debt of gratitude and offer our most sincere thanks. Although the many cited references are authored by members of our science team, each finding depended greatly on the skill and dedication of the development and operations teams as well as our many external collaborators and site hosts.

References

Adamo C, Goodman S, Mugnai A, Weinman JA, Lightning Measurements from Satellites and Significance for Storms in the Mediterranean, ch. 14, this volume.

Burr T, Jacobson A, Mielke A (2004) A global radio frequency noise survey as observed by the FORTE satellite at 800 km altitude. Radio Sci 39(4), DOI 10.1029/2002RS002865

Cummins KL, Murphy MJ, Bardo EA, Hiscox WL, Pyle RB, Pifer AE (1998) A combined TOA/MDF technology upgrade of the U.S. National Lightning Detection Network. J Geophys Res 103(D8):9035–9044

Davis SM, Suszcynsky DM, Light TEL (2002) FORTE observations of optical emissions from lightning: Optical properties and discrimination capability. J Geophys Res 107(D21):4579–4579

Eack KB (2004) Electrical characteristics of narrow bipolar events. Geophys Res Lett 31(20):L20, 102–104

Finke U (2009), Optical Detection of Lightning from Space, ch. 12, this volume.

Hamlin T, Light TE, Shao XM, Eack KB, Harlin JD (2007) Estimating lightning channel characteristics of positive narrow bipolar events using intra-channel current reflection signatures. J Geophys Res 112:D14108, DOI 10.1029/2007JD008471

Holden DN, Munson CP, Devenport JC (1995) Satellite observations of transionospheric pulse pairs. Geophys Res Lett 22(8):889–892

Jacobson AR (2003a) How do the strongest radio pulses from thunderstorms relate to lightning flashes? J Geophys Res 108, DOI10.1029/2003JD003936

Jacobson AR (2003b) Relationship of intracloud lightning radio frequency power to lightning storm height, as observed by the FORTE satellite. J Geophys Res 108, DOI 10.1029/2002JD002956

Jacobson AR, Heavner MJ (2005) Comparison of narrow bipolar events with ordinary lightning as proxies for severe convection. Mon Weather Rev 133(5):1144–1154

Jacobson AR, Light TEL (2003) Bimodal radio frequency pulse distribution of intracloud-lightning signals recorded by the FORTE satellite. J Geophys Res 108(D9), DOI 10.1029/2002JD002613

Jacobson AR, Shao XM (2001) Using geomagnetic birefringence to locate sources of impulsive, terrestrial VHF signals detected by satellites on orbit. Radio Sci 36(4):671–680

Jacobson AR, Shao XM (2002a) FORTE satellite observations of very narrow radiofrequency pulses associated with the initiation of negative cloud-to-ground lightning strokes. J Geophys Res 107(D22), DOI 4610.1029/2001JD001542

Jacobson AR, Shao XM (2002b) On-orbit direction-finding of lightning radiofrequency emissions recorded by the FORTE satellite. Radio Sci 37(4), DOI 10.1029/2001RS002510

Jacobson AR, Knox SO, Franz R, Enemark DC (1999) FORTE observations of lightning radiofrequency signatures: Capabilities and basic results. Radio Sci 34(2):337–354

Jacobson AR, Cummins KL, Carter M, Klingner P, Dupre DR and Knox SO (2000) FORTE radiofrequency observations of lightning strokes detected by the National Lightning Detection Network. J Geophys Res 105:15653–15662

Kirkland MW, Suszcynsky DM, Guillen JLL, Green JL (2001) Optical observations of terrestrial lightning by the FORTE satellite photodiode detector. J Geophys Res 106:33499–33509

Lang TJ, Miller LJ, Weisman M, Rutledge SA, III LJB, Bringi VN, Chandrasekar V, Detwiler A, Noesken N, Helsdon J, Knight C, Krehbiel P, Lyons WA, MacGorman D, Rasumssen E, Rison W, Rust WD, Thomas RJ (2004) The severe thunderstorm electrification and precipitation study. Bull Amer Meteorol Soc DOI 10.1175/BAMS-85-8-1107

Lay EH, Holzworth RH, Rodger CJ, Thomas JN, Pinto O, Dowden RL (2004) WWLL global lightning detection system: Regional validation study in Brazil. Geophys Res Lett 31(L03102), DOI 03110.01029/02003GL018882

Le Vine DM (1980) Source of the strongest RF radiation from lightning. J Geophys Res 85:4091–4095

Lee ACL (1986a) An experimental study of the remote location of lightning flashes using a VLF arrival time difference technique. Q J R Meteorol Soc 112:203–229

Lee ACL (1986b) An operational system for the remote location of lightning flashes using a VLF arrival time difference technique. J Atmos Oceanic Technol 3:630–642

Lehtinen NG, Gorham PW, Jacobson AR, Roussel-Dupré RA (2004) FORTE satellite constraints on ultrahigh energy cosmic particle fluxes. Phys Rev D 69(1), DOI 10.1103/PhysRevD.69.013008

Light TE, Jacobson A (2002) Characteristics of impulsive VHF lightning observed by the FORTE satellite. J Geophys Res 107, DOI 10.1029/2001JD001585

Light TEL, Jacobson AR, Suszcynsky DM (2001) Coincident radio frequency and optical emissions from lightning, observed with the FORTE satellite. J Geophys Res 106:28223–28232

Massey RS (1990) Ionospheric group delay and phase including ionospheric refractive effects. Tech. rep., Los Alamos National Laboratory, Los Alamos, New Mexico

Massey RS, Holden DN (1995) Phenomenology of transionospheric pulse pairs. Radio Sci 30(5):1645–1659

Massey RS, Holden DN, Shao XM (1998a) Phenomenology of transionospheric pulse pairs: Further observations. Radio Sci 33(6):1755–1761

Massey RS, Knox SO, Franz RC, Holden DN, Rhodes CT (1998b) Measurements of transionospheric radio propagation parameters using the FORTE satellite. Radio Sci 33(6):1739–1753

Rison W, Thomas RJ, Krehbiel PR, Hamlin T, Harlin J (1999) A GPS-based three-dimensional lightning mapping system: Initial observations in central New Mexico. Geophys Res Lett 26(23):3573–3576

Rodger CJ, Brundell JB, Dowden RL, Thomson NR (2004) Location accuracy of long distance VLF lightning location network. Ann Geophys 22:747–758, sRef-ID: 1432-0576/ag/2004-22-747

Rodger CJ, Brundell JB, Dowden RL (2005) Location accuracy of VLF World-Wide Lightning Location (WWLL) network: Post-algorithm-upgrade. Ann Geophys 23:277–290, sRef-ID: 1432-0576/ag/2005-23-277

Roussel-Dupré RA, Jacobson AR, Triplett LA (2001) Analysis of FORTE data to extract ionospheric parameters. Radio Sci 36(6):1615–1630

Rust WD, MacGorman DR, Bruning EC, Weiss SA, Krehbiel PR, Thomas RJ, Rison W, Hamlin T, Harlin J (2005) Inverted-polarity electrical structures in thunderstorms in the Severe Thunderstorm Electrification and Precipitation Study STEPS. Atmos Res 76:247–271

Shao XM, Jacobson AR (2001) Polarization observations of broadband VHF signals by the FORTE satellite. Radio Sci 36(6):1573–1589

Shao XM, Jacobson AR (2002) Polarization observations of lightning-produced VHF emissions by the FORTE satellite. J Geophys Res 107(D20), DOI 10.1029/2001JD001018

Shao XM, Jacobson AR, Fitzgerald TJ (2004) Radio frequency radiation beam pattern of lightning return strokes: A revisit to theoretical analysis. J Geophys Res 109, DOI 10.1029/2004JD004612

Shao XM, Harlin J, Stock M, Stanley M, Regan A, Wiens K, Hamlin T, Pongratz M, Suszcynsky D, Light T (2005a) Katrina and Rita were lit up with lightning. EOS Trans, AGU 86(42):398, DOI 10.1029/2005EO420004

Shao XM, Jacobson AR, Fitzgerald TJ (2005b) Radio frequency radiation beam pattern of lightning return strokes: Inferred from FORTE satellite observations. J Geophys Res 110(D24), DOI 10.1029/2005JD006010

Shao XM, Stanley M, Regan A, Harlin J, Pongratz M, Stock M (2006) Total lightning observations with the new and improved Los Alamos Sferic Array (LASA). J Atmos Oceanic Technol 23:1273–1288

Smith DA, Shao XM, Holden DN, Rhodes CT, Brook M, Krehbiel PR, Stanley M, Rison W, Thomas RJ (1999) A distinct class of isolated intracloud lightning discharges and their associated radio emissions. J Geophys Res 104:4189–4212

Smith DA, Eack KB, Harlin J, Heavner MJ, Jacobson AR, Massey RS, Shao XM, Wiens KC (2002) The Los Alamos Sferic Array: A research tool for lightning investigations. J Geophys Res 107, DOI 10.1029/2001JD000502

Smith DA, HeavnerMJ, Jacobson AR, Shao XM, Massey RS, Sheldon RJ,Wiens KC (2004) A method for determining intracloud lightning and ionospheric heights from VLF/LF electric field records. Radio Sci 39, DOI 10.1029/2002RS002790

Suszcynsky DM, Heavner MJ (2003) Narrow bipolar events as indicators of convective strength. Geophys Res Lett 30, DOI 10.1029/2003GL017834

Suszcynsky DM, Kirkland MW, Jacobson AR, Franz RC, Knox SO, Guillen JLL, Green JL (2000) FORTE observations of simultaneous VHF and optical emissions from lightning: Basic phenomenology. J Geophys Res 105(D2):2191–2201

Suszcynsky DM, Light TE, Davis S, Green JL, Guillen JLL, Myre W (2001) Coordinated observations of optical lightning from space using the FORTE photodiode detector and CCD imager. J Geophys Res 106:17897–17906

Suszcynsky DM, Jacobson AR, Linford J, Light TE, Musfeldt A (2005) VHF lightning detection and storm tracking from GPS orbit. In: Annual Mtg., Amer. Meterol. Soc., p Abstract P2.5

Tessendorf SA, Rutledge SA, Wiens KC (2007) Radar and lightning observations of normal and inverted polarity multicellular storms from STEPS. Mon Wea Rev 135:3682–3706

Thomas RJ, Krehbiel PR, Rison W, Hamlin T, Harlin J, Shown D (2001) Observations of VHF source powers radiated by lightning. Geophys Res Lett 28(1):143–146, DOI 10.1029/2000GL011464

Tierney HE, Jacobson AR, Roussel-Dupré R, Beasley WH (2002) Transionospheric pulse pairs originating in marine, continental and coastal thunderstorms: Pulse energy ratios. Radio Sci 27(3), DOI 10.1029/2001RS002506

Weber ME, Williams ER, Wolfson MM, Goodman SJ (1998) An assessment of the operational utility of a GOES Lightning Mapping Sensor. Project Report NOAA-18 MIT Lincoln Laboratory, Lexington, MA 13 February 1998, 108 pp

Wiens KC, Rutledge SA, Tessendorf SA (2005) The 29 June supercell observed during STEPS. Part II: Lightning and charge structure. J Atmos Sci 62:4151–4177

Wiens KC, Hamlin T, Harlin J, Suszcynsky DM (2008) Relationships among narrow bipolar events, "total" lightning, and radar-inferred convective strength in Summer 2005 Great Plains thunderstorms. J Geophys Res 113(D05201), DOI 10.1029/2007JD009400

Willett JC, Krider EP (2000) Rise times of impulsive high-current processes in cloud-to-ground lightning. IEEE Trans Ant Prop 48(9):1442–1451

Willett JC, Bailey JC, Krider EP (1989) A class of unusual lightning electric field waveforms with very strong high-frequency radiation. J Geophys Res 94:16255–16267

Willett JC, Bailey JC, Leteinturier C, Krider EP (1990) Lightning electromagnetic radiation field spectra in the interval from 0.2 to 20 MHz. J Geophys Res 95(D12):20367–20387

Willett JC, Krider EP, Leteinturier C (1998) Submicrosecond field variations during the onset of first return strokes in cloud-to-ground lightning. J Geophys Res 103(D8):9027–9034

Williams ER, Boldi B, Matlin A, Weber M, Hodanish S, Sharp D, Goodman S, Raghaven R, Buechler D (1999) The behavior of total lightning activity in severe Florida thunderstorms. Atmos Res 51:245–264